High-pressure study of silane to 150 GPa

Timothy A. Strobel,[1,*] Alexander F. Goncharov,[1] Christopher T. Seagle,[1,2] Zhenxian Liu,[1] Maddury Somayazulu,[1] Viktor V. Struzhkin,[1] and Russell J. Hemley[1]

[1]*Geophysical Laboratory, Carnegie Institution of Washington, Washington, DC 20015, USA*

[2]*Smithsonian Institution, National Museum of Natural History, Washington, DC 20560, USA*

(Received 17 December 2010; published 7 April 2011)

We present an extensive study of the optical, electronic, and structural properties of silane (SiH_4) to 150 GPa through the use of Raman spectroscopy, optical microscopy, synchrotron infrared reflectivity, optical absorption, and synchrotron x-ray diffraction measurements. To mitigate possible contamination from previously reported metal hydride formation, we performed experiments using gold-lined sample gaskets, finding molecular silane remains in the transparent and insulating $P2_1/c$ structure until ~40 GPa. Silane shows a partial loss of crystallinity above ~50 GPa and appears to visibly darken. The darkening is plausibly the result of a loss of molecular character with many enthalpically competitive pathways available, including decomposition, combined with the absorptive nature of the sample. Above 100 GPa we observed crystallization into structures partially consistent with the previously reported nonmolecular $I\bar{4}2d$ and $I4_1/a$ types. In the absence of decomposition, silane remains partially transparent and nonmetallic to at least 150 GPa with a band gap constrained between 0.6 and 1.8 eV. Under pressure, silane is sensitive to irradiation from x-rays and lasers, and may easily decompose into metallic silicon. We suggest that previous reports of metallization starting from molecular SiH_4 arise from decomposition, and superconductivity may originate from hydrogen-doped silicon. While silane may readily decompose, the inherent metastability provides access to a wide range of path- and sample-history-dependent states and suggests a unique range of physical properties for hydrogen-rich silicon alloys.

DOI: 10.1103/PhysRevB.83.144102 PACS number(s): 81.40.Vw, 61.66.Fn, 62.50.−p, 74.62.Fj

I. INTRODUCTION

The pursuit of superconductivity and novel quantum behavior in light-element systems is of great experimental and theoretical interest,[1–4] fueled largely by predictions of metallization and high-temperature superconductivity in hydrogen, in both paired and monatomic states.[5–8] In 2004, Ashcroft invigorated this interest with the suggestion that hydrogen-dominant metallic alloys could also be high-temperature superconductors.[9] By this argument, covalent hydrides could exhibit metallization at significantly reduced pressures compared with pure hydrogen due to "chemical precompression." That is, covalent hydrides possess a larger average valence electron density compared to bulk hydrogen at equivalent pressure and could also exhibit features important for phonon-mediated high-temperature superconductivity: wide overlapping bands, high density of states, and strong electron-phonon interaction. Ashcroft[9] specifically suggested group-14 hydrides as potential candidates for this behavior and several theoretical and experimental studies followed.

Feng *et al.*[10] used density functional theory (DFT) to determine several energetically competitive structures for silane up to 160 GPa. Silane was suggested to exist as insulating molecular crystals of covalently bonded SiH_4 with tetrahedral coordination of silicon below ~20 GPa. At pressures above 25 GPa, Feng *et al.*[10] determined that sixfold coordinated structures were more favorable and suggested some eightfold coordination at higher pressures. Band gaps were calculated for these structures as a function of pressure and metallization was estimated to occur at 91 GPa (DFT lower estimate) for the most energetically favorable $O3$ structure. The superconducting transition temperature (T_c) for the $O3$ structure was suggested to rise steeply from ~0 K at 91 GPa to 166 K at 202 GPa.

Subsequently, Pickard and Needs[11] used first-principles random structure search methods to determine energetically competitive high-pressure phases of silane to 300 GPa. At low pressure, silane was found to be unstable with respect to decomposition. An insulating chainlike $P2/c$ structure was determined in a small pressure range near 40 GPa. Above 50 GPa a tetragonal $I4_1/a$ structure was calculated to be stable, which then transforms to a monoclinic $C2/c$ structure above 260 GPa. The $I4_1/a$ structure was determined to remain insulating to about 200 GPa and the $C2/c$ structure was predicted to be a good metal with the possibility of high-temperature superconductivity. Pickard and Needs[11] confirmed several structures predicted by Feng *et al.*[10] but found them to be higher-enthalpy phases.

Yao *et al.*[12] used both static and dynamical first-principles calculations to determine the structures and electronic properties of high-pressure silane. The study revealed a novel metallic monoclinic $C2/c$ structure (different from that predicted by Pickard and Needs[11]), metastable with respect to the $I4_1/a$ structure over the same pressure range. However, this energy difference is small and when zero-point energy considerations are taken into account the transformation to the new $C2/c$ structure may be kinetically possible. T_c for the $C2/c$ predicted by Yao *et al.*[12] was estimated to be 45–55 K between 90 and 125 GPa due to a large electron-phonon coupling.

Using a combined experimental and theoretical approach, Degtyareva *et al.*[13] performed a high-pressure structural study on SiH_4. Using powder x-ray diffraction techniques, silane was determined to adopt the $SnBr_4$-type structure ($P2_1/c$) between 11 and 40 GPa: a molecular insulating crystal structure comprised of tetrahedral SiH_4 molecules, common for many other AX_4 species. Above ~25 GPa the appearance of new weak diffraction lines inconsistent with the $P2_1/c$ structure

indicated the onset of a structural phase transition; however, aside from these weak contributions, patterns were indexed and refined to the $P2_1/c$ structure up to 40 GPa. *Ab initio* calculations revealed the $P2_1/c$ structure to be the stable ground-state relative to a cubic F lattice between 2 and 27 GPa. A $P2/c$ structure was calculated to have the lowest enthalpy between 27 and 50 GPa, in reasonable agreement with the work of Pickard and Needs,[11] although experimental diffraction patterns did not support this structure type.

Chen *et al.*[14] measured Raman and infrared (IR) reflectivity on silane up to 70 GPa. Based on Raman measurements, silane was found to freeze at 1.7 GPa and go through a number of phase transitions at ∼4 GPa (silane III), ∼6.5 (silane IV), ∼10 (silane V), and ∼27 GPa (silane VI). These phase transformations were inferred from spectroscopic data, namely, from features in Raman fundamentals (see for example Fournier *et al.*[15]) and observations of frequency shifts with pressure. Phase V, between 10 and 27 GPa, is the same $P2_1/c$ phase measured by Degtyareva *et al.*[13] and samples remained completely transparent below 27 GPa. Above 27 GPa, it was reported in Ref. 14 that silane samples started to darken with increasing pressure, eventually turning completely opaque above ∼30 GPa. The opacity was followed by a loss of Raman signal above 32 GPa. This behavior was not reported by Degtyareva *et al.*,[13] whose diffraction measurements extended to 40 GPa. Chen *et al.*[14] also measured IR reflectivity spectra between 12 and 70 GPa. At low pressure (<40 GPa) the reflectivity spectra were characterized by phonon reflection of the ν_4 bending mode of SiH_4 near 850 cm^{-1}. At higher energy the reflectivity was small (a few percent) and constant, consistent with an insulating molecular solid. With increasing pressure (>55 GPa) a marked increase in the reflectivity over the entire energy range, and specifically a Drude absorption feature where the reflectivity approached unity at the lowest energy, was observed. These observations led to the suggestion that SiH_4 undergoes an insulator-to-metal transition at 60 GPa. The reflectivity spectra were fitted using a classical Drude-Lorentz model with a plasmon frequency comparable to that of Pb at ambient pressure.

Concurrent work by Eremets *et al.*[16] reported that the metallization of silane occurs between 50 and 65 GPa. This conclusion was based on electrical resistance measurements where a sudden drop in resistance was observed at room temperature. In this pressure range the sample was reported to suddenly darken and Raman spectra were no longer detectable. Based on synchrotron x-ray diffraction measurements, Eremets *et al.*[16] suggested that the metallic phase of silane has a structure based on $P6_3$ symmetry and occurs after a 60% volume collapse from the insulating $P2_1/c$ structure. The $P6_3$ structure was reported to persist to pressures of 190 GPa; however, it was concluded that the metallic phase coexists with the transparent insulating $I4_1/a$ phase predicted by Pickard and Needs.[11] The volume of the $I4_1/a$ phase is 25% greater than the $P6_3$ metallic phase at the transition pressure. A superconducting transition with T_c of 17 K at 96 and 120 GPa was reported using electrical resistance measurements.[16] T_c initially increased sharply with pressure from inception at ∼65 GPa, decreased with pressure above 100 GPa, and finally increased again above ∼160 GPa.

Further computational studies were performed by the authors of Ref. 17, who used DFT to calculate the electronic and dynamical properties of compressed silane. They confirmed the molecular insulating $P2_1/c$ structure as the low-pressure ground state and proposed an insulating $Fdd2$ structure between ∼30 and 60 GPa. The stability of the $I4_1/a$ structure between 60 and 220 GPa was predicted. Above 220 GPa, Chen *et al.*[17] found a metallic $Cmca$ layered structure and predicted the metallic $C2/c$ structure above 270 GPa. For the $Cmca$ structure, they calculated a T_c = 20–75 K, which was related to a strong electron-phonon coupling due to phonons involving H-H vibrations. The experimental $P6_3$ metallic structure[16] was calculated to have a high enthalpy relative to other candidates, and phonon calculations revealed it to be dynamically unstable.

DFT calculations by Kim *et al.*[18] also found the $P2_1/c$ and $I4_1/a$ structures as ground states of silane for pressures below 30 GPa and above 50 GPa, respectively. When zero-point motion was considered, a metallic $P4/nbm$ phase became the ground state above 97 GPa and dynamical stability of this phase was observed above 43 GPa. The experimental metallic $P6_3$ structure[16] was suggested to be mechanically unstable, and the $P4/nbm$ structure was considered a more likely candidate for metallic silane.

A joint experimental Raman and x-ray diffraction study of silane up to 70 GPa was performed by Narayana *et al.*[19] Silane solidified at 1.8 GPa and was found to adopt the monoclinic $P2_1/c$ structure between 10-27 GPa. Similar to previous experimental reports,[14,16] initially transparent samples were reported to darken and appear shiny above 27 GPa with simultaneous loss of Raman signal.[19] Samples decompressed from 70 GPa were found to contain both crystalline and hydrogenated amorphous silicon. They suggested that the type of gasket material used may contribute to this observation, finding samples were shinier when a stainless steel gasket was used compared with rhenium or tungsten gaskets. This suggests that silane dissociation may be catalyzed by hydrogen absorption into the gasket material. These observations imply that silicon and molecular hydrogen may be thermodynamically preferred to silane at high pressure.

Martinez-Canales *et al.*[20] used an *ab initio* evolutionary algorithm method for high-pressure structural characterization of silane. The low-pressure structure of symmetry $P2_1/c$ was confirmed, and as in Ref. 17, an insulating structure with $Fdd2$ symmetry was determined above 25 GPa. Several energetically comparable structures were found near 50 GPa. Between 50 and 225 GPa the $I4_1/a$ structure became the ground state and at 225 GPa they suggested a metallic $Pbcn$ phase as the most stable structure. The $Fdd2$ to $I4_1/a$ transition is reconstructive and, with many enthalpically competitive structures at this pressure, the possibility for extended metastability is high. At 190 GPa a T_c of 16.5 K was calculated for the $Pbcn$ structure (metastable with respect to $I4_1/a$ at this pressure). In a related work, Yan *et al.*[21] calculated T_c for the $Pbcn$ structure to be 16.5 K at 188 GPa. Martinez-Canales *et al.*[20] suggested that the metallic $P6_3$ structure is thermodynamically and dynamically unstable.

More recently, Degtyareva *et al.*[22] reported an additional experimental study of silane to 108 GPa. Thermodynamic inconsistency was suggested for the metal-to-insulator transition at ∼100 GPa reported by Eremets *et al.*[16] where a 25%

volume increase was accompanied by two-phase coexistence up to 190 GPa. Degtyareva *et al.*[22] suggested that the metallic $P6_3$ phase reported previously[16] might actually be platinum hydride (Pt was used for electrical resistance measurements) and showed good agreement between diffraction patterns for PtH (Ref. 23) and the $P6_3$ phase[16] as well as good agreement between the unit cell volumes. Silane was suggested to undergo partial decomposition and amorphization above ∼50 GPa based on x-ray diffraction results and the formation of ReH, produced by hydrogen uptake into the Re gasket material, was demonstrated. Above ∼100 GPa silane recrystallized into a high-pressure phase. In addition to pure silane, several similar studies considered germane,[24–27] stannane,[28–30] plumbane,[31] other hydrides,[32–39] and mixtures.[40–49]

From the published theoretical and experimental studies on silane it is clear that a precise understanding of the high-pressure behavior is lacking. Some experimental reports[14,16] claim metallization near 55 GPa, while others[19,22] claim partial decomposition, amorphization, and metal hydride formation. The consensus among computational studies suggests that, while metallization and superconductivity are possible, these structures do not adopt ground-state enthalpies until pressures greater than 200 GPa are reached.[11,17,20] Additionally, the experimentally reported $P6_3$ metallic structure cannot be reconciled with theory.[17,18,20] The reported insulator-to-metal transition at 55 GPa followed by a metal-to-insulator transition at 100 GPa with simultaneous volume increase is highly abnormal.

In the present work, our aim is to address these issues and provide a better fundamental understanding of the high-pressure properties of SiH_4. Additionally, it is important to explore various pathways revealing different thermodynamic and metastable states that may exhibit unique material properties. We present an extensive experimental study on the optical, structural, and electronic properties of silane via Raman spectroscopy, optical microscopy, synchrotron infrared reflectivity, optical absorption, and synchrotron x-ray diffraction measurements. In order to mitigate possible chemical reactions with the gasket material (metal hydride formation), we have conducted our experiments using gold-lined gaskets.

II. METHODS AND ANALYSIS

Studies on SiH_4 were performed using symmetric diamond anvil cells utilizing 100–300 μm anvil culets. Given previous demonstrations of interactions with gasket materials,[19,22] we conducted experiments using gold-lined gaskets, unaware of any gold hydrides in this pressure range at ambient temperature. This eliminates the possibility of reactions with the gasket material. X-ray diffraction was used to observe structural changes in the gold lattice if hydride formation occurred.

A gold liner was formed by compressing a piece of gold wire into a tungsten sample chamber and drilling a slightly smaller hole through the gold. Other experiments were performed using pure tungsten and rhenium gaskets. Pressure was determined by ruby fluorescence,[50] diffraction lines from gold,[51] and from the Raman spectrum of diamond.[52] To avoid direct laser exposure, ruby grains were pressed into the gold lining in order to estimate pressure. SiH_4 (Aldrich, electronic grade) was cryogenically loaded into the cell by condensing solid SiH_4 powder in the gasket hole and cooled in liquid nitrogen in a dry N_2-purged glove box. Once the SiH_4 was loaded, the cell was warmed to ambient temperature and the absence of possible impurities (e.g., N_2, H_2O, Si) was verified by Raman spectroscopy.

A. Raman spectroscopy

Raman spectra were obtained using a Princeton Instruments spectrograph (SP2300) with a 300 mm focal length. The 633 nm line of a HeNe laser and the 488 or 514.5 nm line of an Ar^+ ion laser at various powers were used as excitation sources and focused through an objective lens. Raman scattered light was collected in the backscatter geometry through a 50 μm spatial filter. Two notch filters were used to allow collection up to 100 cm^{-1} from the laser line. Scattered light was focused on a 50 μm slit and dispersed off a 300 or 1500 groove/mm grating onto a liquid-nitrogen-cooled charge-coupled device (CCD) detector.

B. X-ray diffraction

Synchrotron x-ray diffraction measurements were carried out at HPCAT (beamline 16-IDB) and GSECARS (beamlines 13-IDD and 13-BMD) of the Advanced Photon Source, Argonne National Laboratory. A monochromatic beam (∼5 × 5 μm^2) was focused on the sample, and data were recorded on a MAR image plate or MAR CCD. Diffraction data were processed using the FIT2D data analysis program.[53]

C. Infrared reflectivity

Synchrotron infrared reflectivity spectra were obtained between 700 and 8000 cm^{-1} using a Bruker IFS66v/S Fourier transform spectrometer with a Bruker IRscope II at U2A beamline, National Synchrotron Light Source, Brookhaven National Laboratory. For reflectivity, four measurements are required at each pressure. The reflectivity at the diamond-sample interface is given by

$$R_{ds} = \frac{I_{ds}}{I_e}\frac{I_d}{I_0}, \tag{1}$$

where I_{ds} is the power reflected from the diamond-sample interface, I_d is the power reflected from the air-diamond interface (the diamond back plate), I_e is the power reflected from the empty cell (through the diamond at the culet), and I_0 is the power reflected from a polished gold mirror (taken as a perfectly reflecting reference surface).

In order to obtain the most accurate reflectivity measurements possible, we fixed all optical components in place; we did not adjust any component in the entire optical path during the measurements. Two days prior to the scheduled measurement time, we mailed our diamonds to the beamline to obtain reference spectra. Infrared light was focused through the diamond onto the culet, the incident aperture was fixed at ∼20 × 20 μm^2, reflected light was passed through another aperture fixed at ∼20 × 20 μm^2 to a HgCdTe detector, and I_e reference spectra were obtained. A ratiometer was used to normalize the beam current, but we obtained I_e reference spectra as a function of beam current for precaution. We also

obtained back-plate (I_d) spectra as a function of beam current for comparison with the loaded sample data.

With the loaded sample, I_{ds} was obtained by focusing the infrared light onto the sample-diamond interface using the exact same configuration as for the reference spectra. In order to obtain the ratio of I_d/I_0 we used the globar source of a separate spectrometer (Bruker Vertex 80v spectrometer at a newly constructed side station of the U2A beamline) to avoid a nonlinear effect on the detector resulting from the high brightness of the synchrotron source. The ratio of I_d/I_0 was an approximately constant value of 0.19 between 700 and 8000 cm^{-1}; the frequency dependence of the ratio was less than the reproducibility between measurements (<1%).

For analysis of the reflectivity spectra, we assume the form of the dielectric function as

$$\hat{e}(\omega) = \varepsilon_1 + i\varepsilon_2 = \varepsilon_\infty + \frac{f_1\omega_1^2}{\omega_1^2 - \omega^2 - i\gamma_1\omega}, \quad (2)$$

where ε_1 and ε_2 are the real and imaginary parts of the dielectric function, respectively, ε_∞ is the background dielectric constant, and f_1, ω_1, and γ_1 are the strength, frequency, and damping factor of oscillator 1.[54]

The reflectivity data were then fitted through nonlinear regression by treating ε_∞, f_1, ω_1, and γ_1 as adjustable parameters using the relation[55]

$$R_{ds} = \frac{n_d^2 + \sqrt{\varepsilon_1^2+\varepsilon_2^2} - \sqrt{2}n_d\left(\varepsilon_1 + \sqrt{\varepsilon_1^2+\varepsilon_2^2}\right)^{1/2}}{n_d^2 + \sqrt{\varepsilon_1^2+\varepsilon_2^2} + \sqrt{2}n_d\left(\varepsilon_1 + \sqrt{\varepsilon_1^2+\varepsilon_2^2}\right)^{1/2}}. \quad (3)$$

D. Optical absorption

Optical absorption measurements (~10 000–30 000 cm^{-1}) were performed on selected samples subsequent to x-ray diffraction and IR reflectivity measurements. Light from a halogen-deuterium lamp was passed through a fiber and focused onto the sample. Transmitted light was collimated with a 20 μm pinhole and passed to a CCD detector. It was not possible to obtain reference spectra from the diamonds used as they broke after the measurements, so we approximated the reference spectra using similar diamonds with the same optical configuration. We obtained measurable absorption signal between ~1.2 and 2.8 eV depending on the sample.

In order to estimate the magnitude of the band gap from the optical absorption spectra, we assumed both direct and indirect interband transitions associated with the steeply rising absorption components. Proportionality of the absorption coefficient α for a direct inter-band transition can be expressed as

$$\alpha(h\nu) \propto (h\nu - E_g)^{1/2}, \quad (4)$$

where $h\nu$ is the photon energy and E_g is the gap energy. The expected behavior for an indirect gap follows

$$\alpha(h\nu) \propto (h\nu - E_g \pm h\Omega)^2, \quad (5)$$

where the difference $\pm h\Omega$ depends on whether a phonon is absorbed or emitted.[54] The nature and magnitude of the gap were estimated by examining plots of $(\alpha d h\nu)^2$ and $(\alpha d h\nu)^{1/2}$ vs $h\nu$ (where d is the sample thickness) and by examining how the maximum measurable absorption shifted as a function of pressure.

III. RESULTS AND DISCUSSION

A. Thermodynamic stability

At standard conditions (298.15 K, 1 atm) the Gibbs free energy of formation for silane is +56.9 kJ/mol.[56] Thermodynamically, the molecule exists metastably with respect to its formation components (Si and H_2), although the molecule possess some degree of chemical stability. Pressure may influence the thermodynamic stability through contributions to the free energy via the PV term. At constant temperature one can determine this influence by correcting the Gibbs free energy of formation through

$$\Delta G_f = \Delta G_f^0 + \int_{P_0}^{P} \Delta V dP. \quad (6)$$

Figure 1 shows the equations of state for silane and formation components, together with the Gibbs free energy of formation of silane as a function of pressure between 0 and 30 GPa (see also Ref. 19). In this analysis, we used the solid phase silane equation of state from Degtyareva *et al.*[13] the solid phase H_2 equation of state from Hemley *et al.*[57] and the Si equation of state determined from the data of Olijnyk *et al.*[58] and McMahon *et al.*[59] At low pressure we compiled fluid phase H_2 data from Lemmon *et al.*[60] and Hermes *et al.*[61] In the absence of thermodynamic PVT data for silane at low

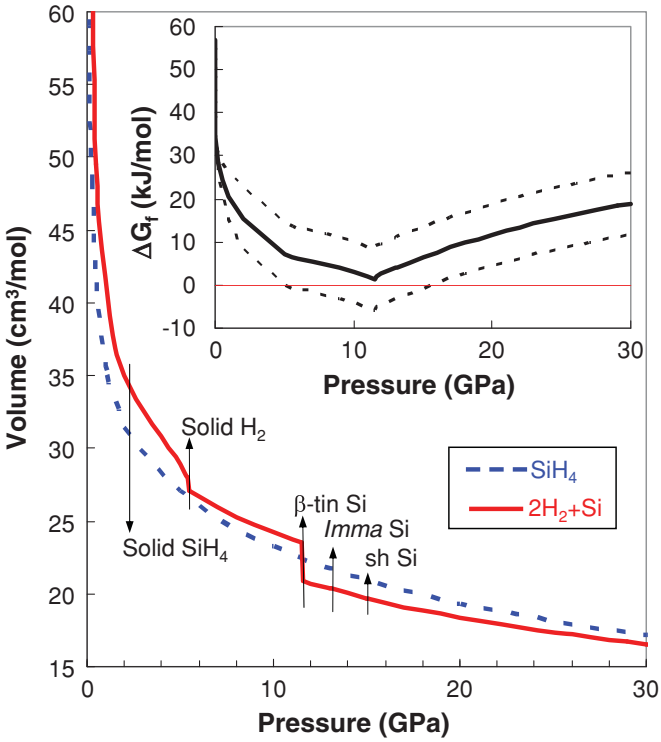

FIG. 1. (Color online) Equations of state for silane and hydrogen plus silicon as a function of pressure. The inset shows the estimated Gibbs free energy of formation at 298 K as a function of pressure, where the dotted lines indicate the range provided for a ±10% variation in the low-pressure silane volume.

pressure, we have assumed that the compressibility of silane is similar to that of methane at the same reduced temperature and pressure (corresponding states), and derived the silane compressibility from methane data.[60] The largest uncertainty in ΔG_f arises from uncertainty in the silane equation of state at low pressure; therefore, we have estimated ΔG_f with a $\pm 10\%$ variation in the silane volume for this pressure range. Estimates of the molar volume of CH_4 between 0.0001 and 0.5 GPa via corresponding states with nitrogen showed an average absolute deviation of 1.0% from accepted values.[60]

Our estimation indicates that silane tends to remain thermodynamically unstable with respect to decomposition over a wide range of pressure. A small pressure window exists between 6 and 16 GPa where thermodynamically stable silane falls within the $\pm 10\%$ volume range, and above 16 GPa, silane becomes unstable again with respect to decomposition. The low-pressure thermodynamic instability from this simple analysis agrees well with first-principles calculations[11] and highlights the imperative realization that prior to embarking on any experimental measurements, one must first acknowledge the reality that SiH_4 is unstable with respect to $Si + 2H_2$ over a large range of pressure. Thus it is pertinent to determine the experimental pressure range over which silane may be maintained, and to determine how the stability is influenced by experimental probes, i.e., high-energy lasers and x-rays. These questions must be reconciled with the previous reports of opacity near 30 GPa and metallization near 55 GPa.

B. Raman spectroscopy and x-ray diffraction

Figure 2 shows Raman spectra of silane in the Si-H stretching region as a function of pressure. We used the 632 nm line of a HeNe laser (<30 mW) as an excitation source. Compared with higher energy lasers, HeNe photons present a smaller chance for radiation-induced damage. Raman spectra obtained are consistent with the earlier reports;[14,16] however, we observed that silane can remain completely transparent to at least 37 GPa with no indication of discoloration. The Si-H stretching mode decreases in frequency with increasing pressure, showing softening, and may indicate instability at higher pressure. During decompression changes in the Raman spectra were reversible, i.e., no decomposition occurred. In contrast, complete sample opacity at 32 GPa was reported in earlier experiments.[14] We suggest that laser-induced decomposition may be at least partially responsible for the previously observed opacity; however, samples may begin to darken under transmitted light over a range of pressure rather than at a distinct point.

To test the laser damage hypothesis, the sample at 37 GPa was exposed to a ~5 mW power (focused though a 20× objective lens) 488 nm Ar^+ laser beam for one second. Figure 2 shows the result of this process where the exposed area immediately turned black. This implies that laser-induced decomposition of silane is possible in this pressure range, and that previous investigators may have unintentionally decomposed the sample. In addition to the laser measurements, we made similar observations with x-rays. After short exposures to synchrotron x-ray beams, we observed previously transparent samples begin to darken, and observed the appearance of crystalline silicon in diffraction patterns.

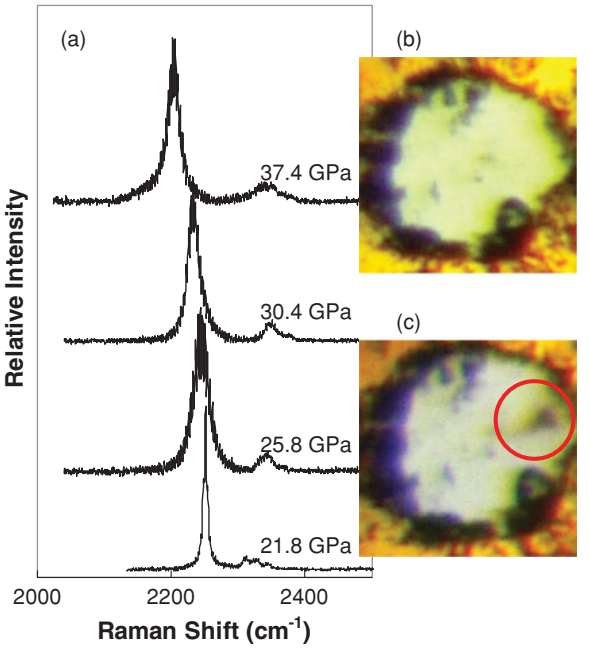

FIG. 2. (Color online) (a) Raman spectra in the Si-H stretching region of silane to 37 GPa using a HeNe laser as excitation source. The sample is contained in a gold-lined gasket with pieces of ruby for pressure calibration. Oscillations in the spectra are an artifact of a beam splitter used for the measurements. Silane sample at 37 GPa before (b) and after (c) exposure to a ~5 mW 488 nm Ar^+ laser for 1 s. Clear damage to the sample occurred after the 1 s exposure [circled in (c)]. The sample chamber is about 50 μm in diameter.

In the region between 6 and 40 GPa most diffraction patterns obtained from samples were successfully indexed to the monoclinic $P2_1/c$ structure in agreement with the results of Degtyareva *et al.*[13] and Narayana *et al.*[19] Figure 3 shows a representative pattern obtained at 8.5 GPa and the Le Bail fit using the $P2_1/c$ structure from Degtyareva *et al.*[13] showing excellent agreement. Unit cell volumes obtained between 6 and 40 GPa were within 2.0% of those obtained by Degtyareva *et al.*[13] Chen *et al.*[14] proposed numerous phase transitions in silane between 4 and 10 GPa based on observations of frequency discontinuities in Raman spectra. Our lowest-pressure diffraction patterns at 6 GPa are explained by the structure of phase V (at pressures where phase III should be stable). Figure 3 clearly shows the phase V structure at only 8.5 GPa. However, in some diffraction patterns we observed a few lines that could not be indexed to the $P2_1/c$ structure, perhaps originating from a small amount of a residual lower-pressure phase. Our diffraction data could be consistent with the boundaries reported previously[14] if the lower-pressure phases are isostructural with phase V. A future crystallography study detailing the low-pressure silane structures is warranted.

Our structural observations in the low-pressure regime (below 40 GPa) were consistent regardless of the gasket material used. Both gold-lined and pure tungsten or rhenium gaskets provided similar results. However, we did observe x-ray-induced decomposition in a few of our samples by the appearance of crystalline silicon. The appearance of silicon in the low-pressure regime was not systematic with gasket

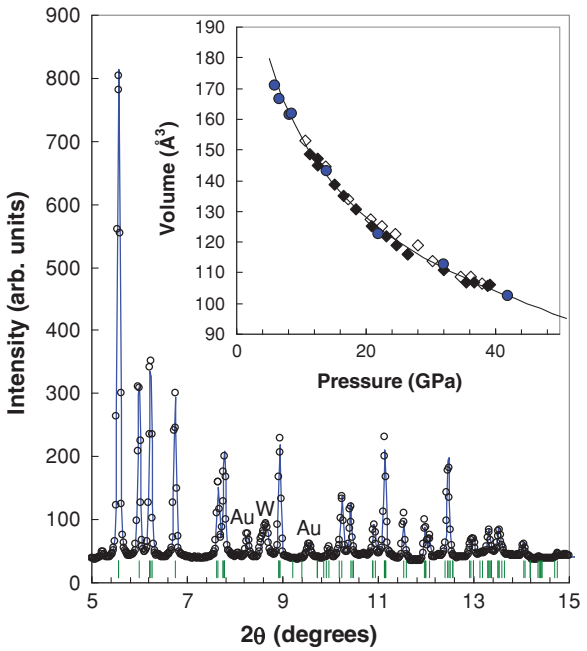

FIG. 3. (Color online) Synchrotron x-ray diffraction pattern ($\lambda = 0.3344$ Å) obtained at 8.5 GPa and room temperature with Le Bail fit. Tick marks indicate allowed reflections for $P2_1/c$ structure with lattice parameters $a = 6.3135(5)$ Å, $b = 4.1613(2)$ Å, $c = 6.3583(2)$ Å, and $\beta = 104.373(5)^\circ$. Inset shows the volume obtained as a function of pressure (circles) compared to results of Ref. 13 (diamonds).

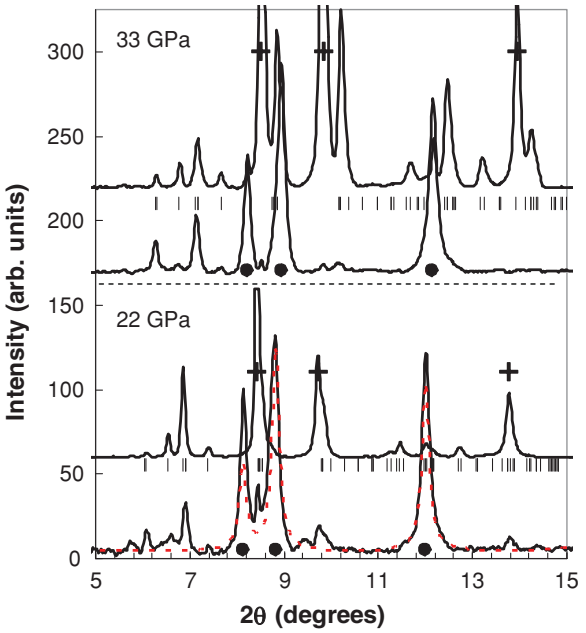

FIG. 4. (Color online) Synchrotron x-ray diffraction of silane ($\lambda = 0.3344$ Å) obtained at 22 GPa (bottom panel) and 33 GPa (top panel). Two patterns from different regions of the sample are shown at each pressure. The dashed profile in the lower panel is a simulated pattern for Si-V. Allowed reflections for Si-V and gold are denoted by circles and crosses, respectively, while reflections for $P2_1/c$ silane are shown by tick marks.

material and was not observed at pressures below ~20 GPa. The appearance of silicon may be correlated with the amount of x-ray exposure. Figure 4 shows diffraction patterns at 22 and 33 GPa with phase V of silicon present. This particular sample was irradiated with x-rays ($\lambda = 0.3344$ Å) for 35 exposures, each lasting 120 s, at 8.5 GPa prior to compression to 22 GPa, yet crystalline Si was not detectable at 8.5 GPa.

The observation of crystalline Si was commensurate with premature darkening of the sample. At 22 GPa the sample turned entirely black and strong diffraction from Si-V was observed in a non-uniform distribution throughout the sample volume. Crystalline silicon coexisted with solid silane, suggesting partial decomposition in this pressure range. In the absence of laser or x-ray exposure, samples tended to remain transparent to higher pressures although the blackening phenomenon may occur over a range of pressure, suggesting that local sample stress may play a role. These results, combined with the laser damage observed (Fig. 2), suggest that the color change of the samples can be related to (partial) decomposition. Phase V of silicon is metallic and does not transmit visible light at the sample thicknesses studied.

C. Higher-pressure x-ray diffraction

Up to ~40 GPa we were able to index diffraction patterns to the molecular monoclinic $P2_1/c$ structure in the absence of observable decomposition. At low pressures we observed strong and sharp diffraction peaks (cf. Fig. 3), but with increasing pressure, the quality of the patterns gradually deteriorated. At 50 GPa, a sparse number of peaks consistent with the $P2_1/c$ structure were observed with weak intensity. Diffraction patterns between 33 and 80 GPa are displayed in Fig. 5.

Above 50 GPa, diffraction patterns were not homogeneous throughout the samples. In some sample regions no detectable diffraction was observed besides that from the gold gasket, suggesting a loss of crystallinity above 50 GPa. This observation is consistent with the previous claim of (partial) pressure-induced amorphization,[22] although we did not observe distinct diffuse scattering beyond the background level. The loss of crystallinity with partial decomposition and amorphization or polymerization has been reported previously for molecular systems such as H_2S.[62,63] Solids containing related tetrahedral molecules like $SnBr_4$, SnI_4, and GeI_4 are reported to undergo pressure-induced amorphization transitions.[64–67]

While some sample regions above 50 GPa displayed no detectable diffraction, weak reflections were observed in other locations, indicating at least partial crystallinity. At 57 GPa the most notable features were two peaks situated at $d = 2.488$ Å (7.71°) and $d = 2.380$ Å (8.06°) for the crystalline regions of the sample. These peaks moved to lower d spacing with pressure and were observed at almost every pressure point up to 80 GPa (Fig. 5).

These two reflections are not consistent with the hcp phase of silicon stable in this pressure range, suggesting that decomposition did not occur. It is unlikely that these lines originate from a gold hydride structure as they were not observed in all patterns, whereas pure gold lines were; one would expect hydride to form around the gasket-sample periphery. The two reflections could be related to the hexagonal

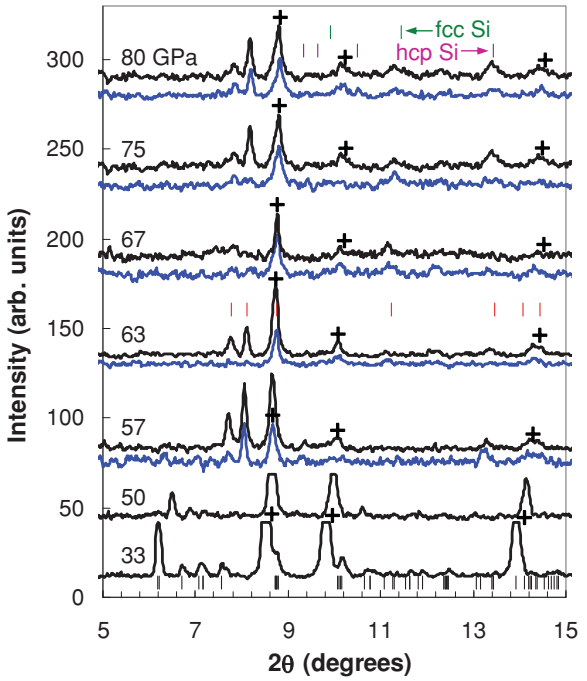

FIG. 5. (Color online) Silane diffraction patterns ($\lambda = 0.3344$ Å) between 33 and 80 GPa. Multiple patterns at the same pressure represent different locations in the cell. At 33 GPa patterns were indexed to the $P2_1/c$ structure (lower tick marks) and traces of this phase remained up to 50 GPa. Tick marks in the middle of the figure represent allowed reflections for space group $P6_3$ with $a = 2.85$ Å and $c = 4.73$ Å. Tick marks for allowed reflections from hcp and fcc silicon at 80 GPa are labeled at the top of the figure. Crosses indicate gold reflections.

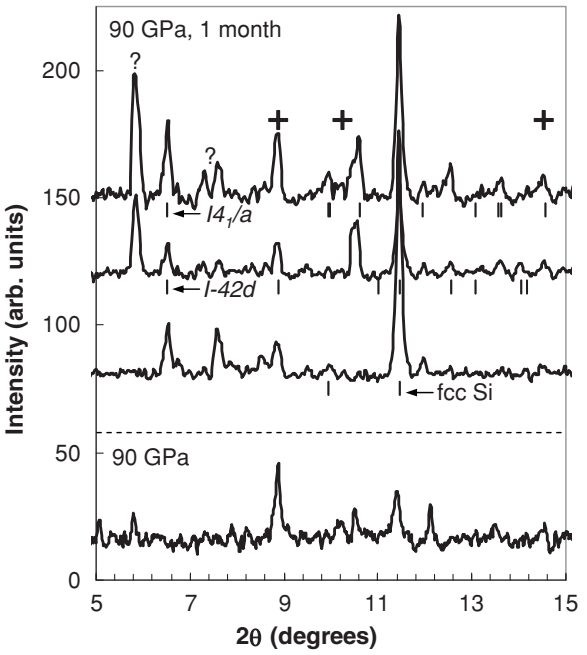

FIG. 6. Diffraction patterns ($\lambda = 0.3344$ Å) of silane at 90 GPa. The lowest pattern was obtained immediately following the measurements in Fig. 5. The upper three patterns were obtained one month later from various locations of the sample volume. Tick marks for fcc silicon as well as the $I\bar{4}2d$ and $I4_1/a$ phases are labeled. Crosses indicate positions for gold reflections at 90 GPa. We were unable to index several of the reflections indicated by "?."

structure reported previously[16] in this pressure range. At 63 GPa these reflections can be indexed with a hexagonal lattice of $a = 2.85$ Å and $c = 4.73$ Å, yielding a volume of 33.3 Å^3 compared with 30 Å^3 for the reported $P6_3$ structure at 51 GPa.[16] We note, however, that the proposed $P6_3$ structure was calculated to be highly dynamically unstable,[18,20] even if in thermodynamic terms it can be metastably maintained. Near 50 GPa, several energy-competitive structures have been predicted,[20] indicating a large susceptibility to structural metastability in this pressure range. The coordination of silicon is expected to increase with pressure and, in addition to a wide range of energetically competitive crystal structures, the formation of semi- or nonmolecular phases including disilane and higher-order polymers may be possible. We compared our diffraction results with theoretically predicted structures,[10,11,20] but were unable to locate a crystal structure that adequately describes these data.

Above ~70 GPa we observed some reflections that are consistent with those of the high-pressure hcp and fcc silicon phases,[58,68] respectively. After one month we observed several new peaks at 90 GPa, although the quality of the patterns remained poor (Fig. 6). One strong reflection observed in all regions of the sample at $d = 1.677$ Å (11.44°) is consistent with the presence of fcc silicon. Several remaining lines are in good agreement with the tetragonal $I\bar{4}2d$ and $I4_1/a$ silane structures originally predicted by Pickard and Needs.[11] The $I4_1/a$ phase was identified as the high-pressure insulating phase by Eremets *et al.*[16] (after the metallic $P6_3$ phase). We note that Eremets *et al.*[16] observed the formation of this phase to be slow, involving only part of the sample after several days. In order to obtain quality data on this phase, Eremets *et al.*[16] annealed the sample for several hours at $T > 400$ K. The slow crystallization of this phase is consistent with our results and indicates the presence of a moderate energy barrier and, possibly, a reconstructive transformation. Similarly, the $I4_1/a$ phase, in coexistence with the $I\bar{4}2d$ phase, was recently observed by Hanfland *et al.*[69] after the sample passed through the amorphous state; the $I4_1/a$ phase was also observed to form from pure silicon and hydrogen above 100 GPa.

Following the diffraction measurements, we obtained Raman spectra of the sample at 90 GPa (Fig. 7). The two modes observed at 1040 and 1920 cm^{-1} agree well with high-pressure Raman spectra for the insulating $I4_1/a$ phase reported[16] at equivalent pressures. This observation supports the high-pressure crystallization of this phase, which likely coexists with other related structures.

D. Infrared reflectivity

Synchrotron IR reflectivity spectra at the diamond-sample interface as a function of pressure to 150 GPa are shown in Figure 8. The low-pressure IR reflectivity of silane is consistent with the previous report.[14] Silane displays minimal reflectivity (~1.0%) between 1500 and 8000 cm^{-1}. This is consistent with the transparent, insulating, and molecular nature of the solid. At lower energy, low-pressure IR reflectivity spectra are characterized by phonon structure with a strong mode at

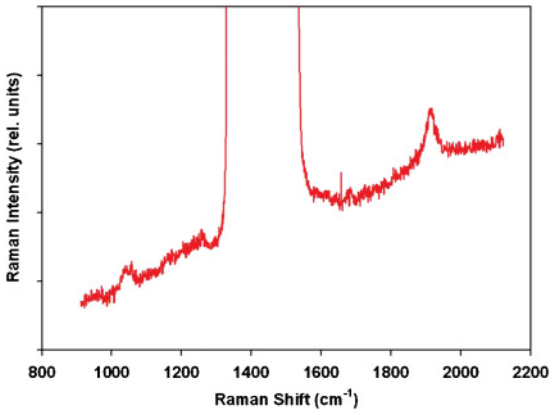

FIG. 7. (Color online) Raman spectrum of SiH_4 sample at 90 GPa after x-ray diffraction measurements. The modes observed at 1040 and 1920 cm^{-1} agree well with frequencies reported in Ref. 16 for the $I4_1/a$ structure at this pressure.

~860 cm^{-1}. We assign the latter feature to the ν_4 bending mode based on the previous assignment from reflectivity measurements,[14] and on consistency with ambient-pressure, low-temperature IR absorption measurements.[15] At low-temperature, phase II of solid silane shows at least five absorption features in the ν_4 region between ~870 and 890 cm^{-1}.[15] This region was fitted with multiple contributions for the high-pressure phases in the previous study.[14] We expect multiple components in this region, yet fitted our spectra with only a single oscillator.

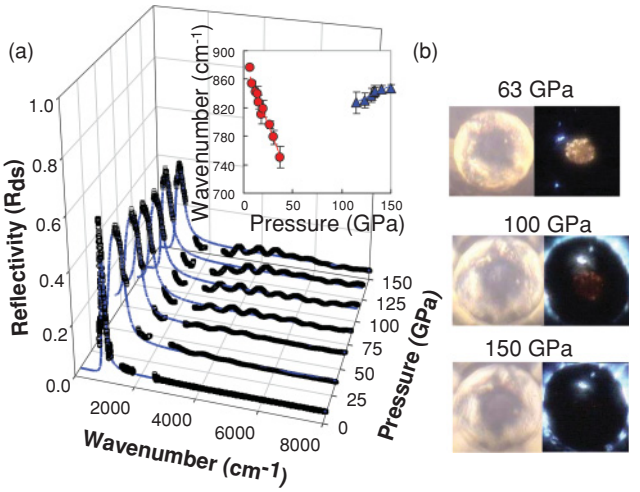

FIG. 8. (Color online) (a) Synchrotron IR reflectivity at the diamond-silane interface as a function of pressure. Lines show best-fit regressions to the experimental data (points). The nitrogen defect impurity and diamond multiphonon absorption regions are removed. Oscillations in the spectra are due to interference fringes between the two parallel diamond surfaces. Reproducibility of reflectivity from repeat measurements was within 5%. The inset shows the frequency of maximum reflectivity in the ν_4 region as a function of pressure. (b) Photomicrographs obtained in reflection (left) and transmission (right). Integration time on the CCD camera was several seconds. Measurable transmission of visible light was found through the sample at 150 GPa.

With increasing pressure the position of the ν_4 reflection (average position with respect to all comprising components) initially decreased in frequency. This softening behavior was also observed previously[14] and may be a harbinger of instability in the silane crystal structure. The average position of the ν_4 mode with pressure is shown in Fig. 8 (inset). As pressure was increased our samples remained transparent until ~40 GPa and then began to visibly darken and appeared black in transmitted white light. Above 40 GPa some light was transmitted through the sample; however, this was only observable through a microscope when the incident intensity was at maximum. At even higher pressure, we were able to observe transmitted white light by collecting images with integration times of several second on the CCD camera—under these conditions silane appeared orange.

The general features of the IR reflectivity spectra showed minimal changes with further application of pressure. Between 1500 and 8000 cm^{-1} the reflectivity increased slightly from ~1% at 15 GPa to ~7% at 150 GPa (Fig. 8). Between 50 and 100 GPa, the ν_4 mode softened to the edge of the detectable frequency range for our measurements; thus our confidence in the peak position decreased in this pressure region. While spectra between 50 and 100 GPa were described well by a single oscillator near 800 cm^{-1}, we observed no definitive peak maximum in this pressure range. This may be consistent with the loss of crystalline or molecular character in this pressure regime as reported previously[22] (and supported by our x-ray diffraction results). Nevertheless, we observed neither an abrupt increase in reflectivity nor a Drude-like absorption feature in the pressure regime previously reported for silane metallization.

Figure 9 shows the reflectivity at 4000 cm^{-1}. At low pressures the two data sets agree well, with the reflectivity at 4000 cm^{-1} being on the order of a couple of percent. The data of Chen *et al.*[14] show an abrupt increase in reflectivity above 50 GPa, approaching 60%, whereas the new data show

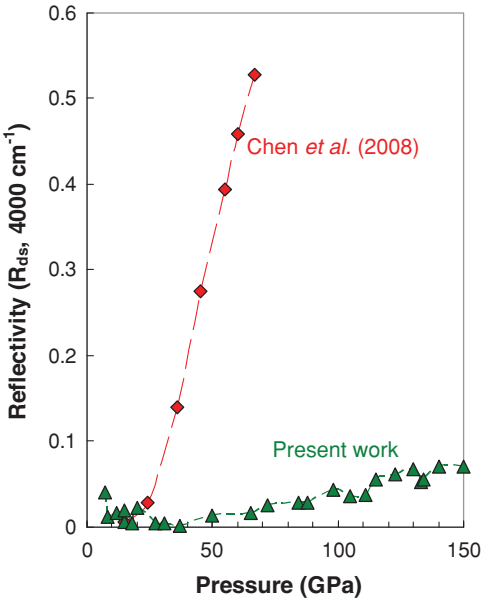

FIG. 9. (Color online) IR reflectivity at the diamond-sample interface at 4000 cm^{-1} compared with data of Ref. 14.

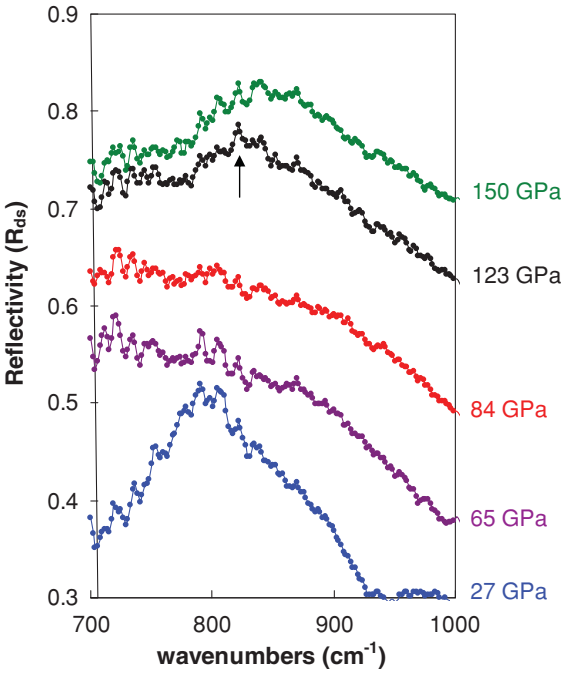

FIG. 10. (Color online) IR reflectivity spectra of silane at the diamond-sample interface between 700 and 1000 cm^{-1} as a function of pressure. The arrow shows the reappearance of the maximum in the ν_4 region. At 27 GPa the reflectivity is presented as obtained. Each data set above 27 GPa is shifted upward by an additional 0.1 units for clarity.

a gradual increase, approaching only 10% at 150 GPa. At 800 cm^{-1} earlier data[14] diverge above 50 GPa and abruptly increase to 100%, whereas our data decline slightly with pressure from 55% to 40% over twice the pressure range.

Above 100 GPa the maximum in the ν_4 bending region reappears (Fig. 10). The appearance of this mode is consistent with previous reports of high-pressure recrystallization and with our x-ray diffraction results which show new lines above ~90 GPa. These results are consistent with a loss of crystalline (and possibly molecular) character above 50 GPa and the formation of new structures above 100 GPa.

Nonlinear regression of the experimental reflectivity data using Eqs. (2) and (3) provided estimates of the frequency-dependent dielectric constant as a function of pressure (Fig. 11). Like the reflectivity data, no significant changes in the dielectric function were observed over the entire pressure range. Substantial changes would be expected for a "polarization catastrophe" affiliated with an insulator-to-metal transition.

Subsequent to IR reflectivity measurements, we obtained synchrotron x-ray diffraction patterns of the sample to determine the structure. Gold diffraction from the gasket indicated a pressure of 145 GPa, and we observed very weak diffraction above the background level. Only two diffraction lines aside from gold were observed and were consistent with the $I4_1/a$ structure with expanded lattice parameters from those reported by Eremets *et al.*[16] at 160 GPa. Additionally, we collected Raman spectra from the sample and observed modes at 2050 and 1160 cm^{-1}, similar to spectra reported for the $I4_1/a$ structure[16] (analogous to Fig. 7).

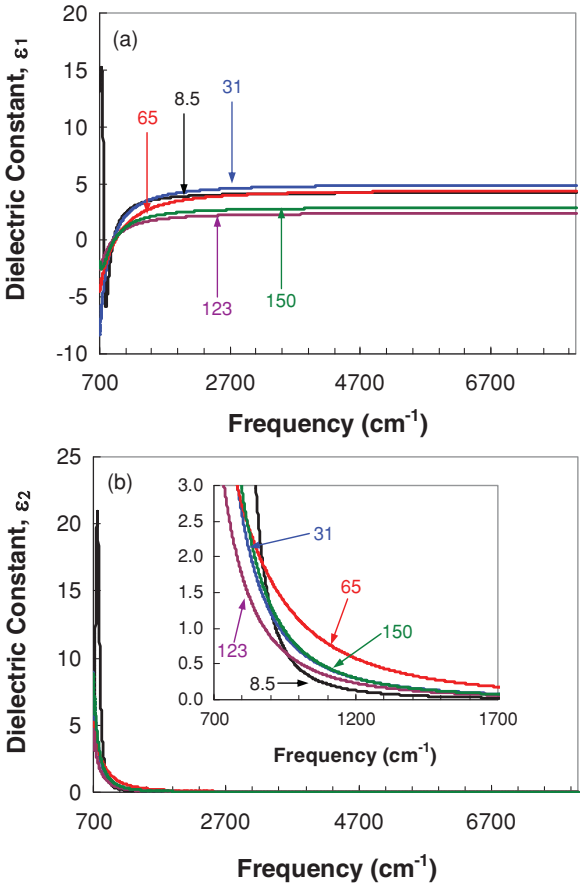

FIG. 11. (Color online) (a) Real and (b) imaginary parts of the dielectric function for SiH_4 at various pressures (indicated on figure in GPa).

E. Optical absorption

While our synchrotron infrared reflectivity data do not support the pressure-induced metallization of silane, and are not consistent with the previous metallization reports,[14,16] we cannot absolutely rule out the presence of a metallic state on the basis of these data alone. We did not measure below 700 cm^{-1} and an indirect band gap closure could possibly allow for some transmitted light (as for metallic xenon[70]). To better quantify the electronic structure of silane, we performed optical absorption measurements as a function of pressure. These results and corresponding photomicrographs are shown in Fig. 12.

Above 50 GPa, the absorption spectra are characterized by an increase in absorption at higher energy with an absorption tail at lower energy. The observation of an absorption edge indicates that valence and conduction bands are not overlapping, i.e., samples are not metallic. At 55 GPa, samples appeared dark in color, with some transmission of visible light possible (Fig. 12). We did not observe the appearance of a shiny metallic luster. Under intense white light, samples appeared orange at 55 GPa and turned reddish with increased pressure. Sample darkening has been reported for other molecular crystals upon polymerization-amorphization transitions even though band gaps are still well within the ultraviolet,[71,72] and the darkening of silane samples above 55 GPa is consistent with the absorptive nature of the samples.

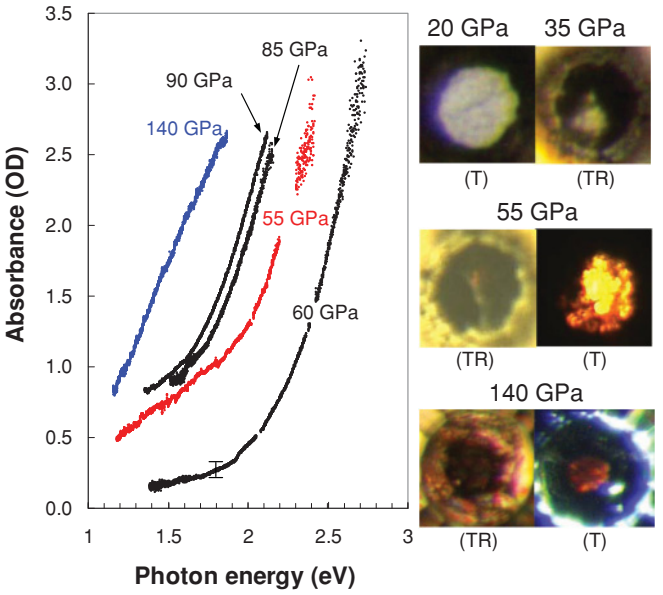

FIG. 12. (Color online) Optical absorption measurements for silane samples at different pressures and sample microphotographs. Spectra at 60, 85, and 90 GPa were obtained from the same sample. The spectra at 55 and 140 GPa were both from separate samples with different thicknesses. A representative error bar is shown in the 60 GPa spectrum. Images are shown for transmission + reflection (TR) and transmission (T). The transmission images at 55 and 140 GPa required several seconds of integration time to obtain.

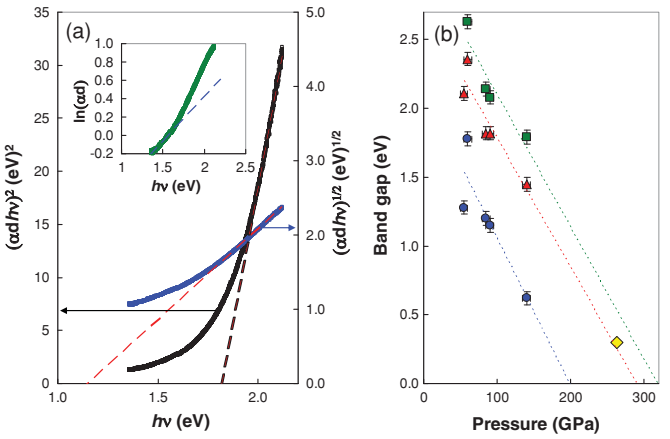

FIG. 13. (Color online) (a) Plots of $(\alpha dh\nu)^2$ and $(\alpha dh\nu)^{1/2}$ versus $h\nu$ at 90 GPa. The intersection of the extrapolated linear portion of the curve with the abscissa represents band gap estimates for direct and indirect transitions. Inset shows Urbach plot with exponential scaling on different energy scales. (b) Estimated SiH_4 band gap with pressure. The actual gap is constrained by indirect estimate (circles), direct estimate (triangles), and maximum absorption estimate (squares). The gap estimate for the $I4_1/a$ structure from Ref. 11 is shown as the diamond.

While the range and quality of the absorption data are not ideal, these data were used to approximate the magnitude of the band gap. We assumed both direct and indirect interband transitions associated with the steeply rising absorption components in Fig. 12. The absorption coefficient α for a direct interband transition is expected to be proportional to the square root of the photon and gap energy difference, whereas an indirect gap is expected to display a squared dependence.[54] A plot of $(\alpha dh\nu)^2$ and $(\alpha dh\nu)^{1/2}$, where d is the sample thickness, versus $h\nu$ can be used to help elucidate the transition mechanism and estimate the gap magnitude. We also estimated the magnitude of the gap by observing the shift in the maximum absorption (optical density $\sim$2.5) with pressure.

Unfortunately, data were obtained over a limited energy range and the nature of the interband transition mechanism is ambiguous; higher-energy linear regimes can be observed for both direct-gap parabolic-band and indirect-gap (Tauc[73]) types of plots [Fig. 13(a)]. Additionally, there is some indication for an Urbach-like absorption regime at lower energy [Fig 13(a) inset] consistent with sample disorder. The assumptions of direct and indirect transitions are likely poor as they pertain strictly to pristine materials. Here our samples contain a mixture of phases as indicated by diffraction measurements. Nevertheless, we are able to constrain the magnitude of the band gap which likely falls somewhere between the indirect-band-gap extrapolation and maximum absorption extremes, and signifies some representative value for the silane phases present.

From these absorption data, we estimate the band gap of SiH_4 to be constrained between 1.3 and 2.6 eV at 55–60 GPa [Fig. 13(b)]. In this pressure range the nature of the solid is ill defined and it is likely that a mixture of phases coexist, possibly including disilane and other higher-order polymers. The magnitude of the energy gap decreased with pressure and at 140 GPa we confine the gap between 0.60 and 1.8 eV. In this pressure range our diffraction patterns were partially consistent with the $I4_1/a$ structure. Pickard and Needs[11] calculated this phase to be insulating up to 200 GPa and at 263 GPa this phase was predicted to be semimetallic with an indirect band overlap of 0.3 eV. A linear extrapolation of our estimated energy gaps places closure between 200 and 320 GPa [Fig. 13(b)], in reasonable agreement with the DFT calculations. We also note that no sharp discontinuities were observed in the highest-pressure IR reflectivity spectra below 1.0 eV (8000 cm^{-1}), suggesting that E_g is greater than this energy at 150 GPa.

F. Silane decomposition and metallic silicon

We have clearly demonstrated that silane may be damaged and undergo partial decomposition, so we must consider the possibility that previous claims of metallization were due to Si rather than SiH_4. In order to address this question we performed a series of experiments where silane was intentionally decomposed through heating. Comparison between samples with intentional decomposition and previous work may help elucidate the role of silicon in sample properties.

Using gold-lined gaskets, we compressed silane to 30 GPa. Samples remained completely transparent and neither x-ray nor Raman measurements were performed to avoid damaging the sample. Once the sample was at 30 GPa, we gently heated the cell to $\sim$100 °C with an external heat source. Almost instantly, a black spot appeared in the center of the sample. The appearance in the center of the sample indicates that the decomposition was not prompted by interaction with the gasket material, but rather likely occurred at the point of highest

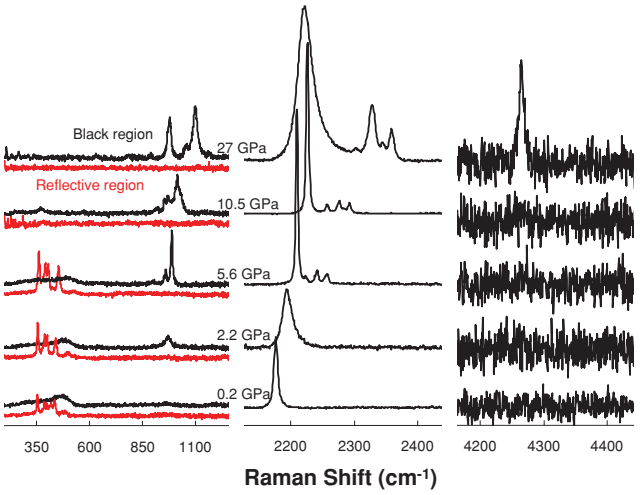

FIG. 14. (Color online) Raman spectra obtained from intentionally decomposed silane sample during decompression. The low-frequency panel shows spectra obtained from black regions of the sample (upper) and spectra obtained from reflective regions of the sample (lower). No Raman signal was observable for the reflective sample regions at higher frequency.

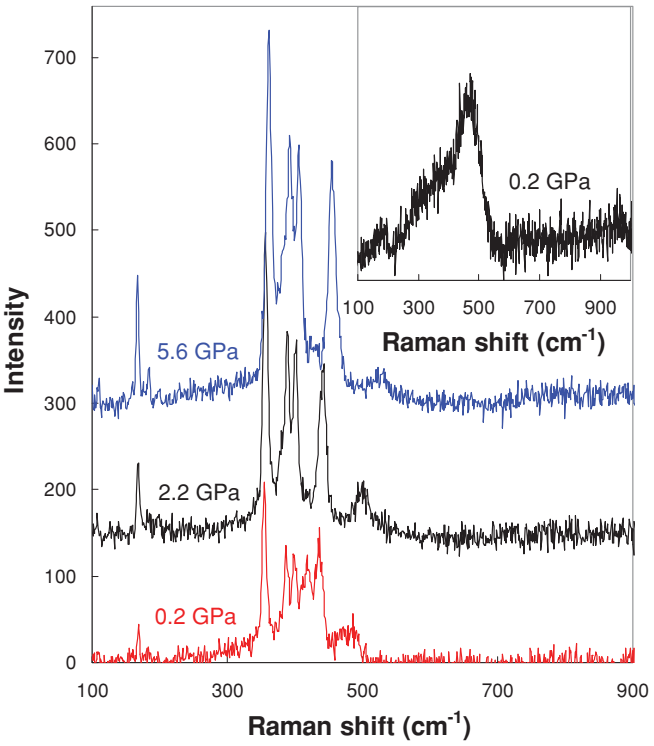

FIG. 15. (Color online) Raman spectra obtained from reflective region upon decompression. (Inset) Black region showing amorphous hydrogenated silicon.

local stress, i.e., the sample center. Over a period of five minutes the entire sample turned black. Ten minutes later, shiny reflective veins began to appear within the sample. When the sample cooled back to ambient temperature, we compared the visual characteristics with those reported by Chen *et al.*[14] It is interesting that our intentionally decomposed silane sample appears nearly identical to the image provided by Chen *et al.*[14] where metallization was claimed. We note that when samples are compressed in gold-lined gaskets in the absence of heating or x-ray or laser exposure, samples still appear dark, but remain at least partially transparent and show no signs of metallic-looking veins. Photomicrograph images of the silane decomposition process are provided as supplemental material.[74]

In order to determine the reaction products from the heated sample, we obtained Raman spectra (Fig. 14). After the sample cooled to room temperature the pressure equilibrated to 27 GPa, likely due to slight thermal expansion of the cell during heating with some hysteresis. We distinguish the Raman spectra into two separate regions: (1) the black areas that do not reflect light and (2) the shiny metallic-looking regions that do reflect light. At 27 GPa the reflective regions of the sample did not have any measurable Raman spectrum. The black regions consisted of molecular silane and a small amount of molecular hydrogen, indicating partial decomposition. Differences in the Si-H stretching and bending regions compared with pristine samples at similar pressure (cf. Fig. 2) indicate new chemical environments and the possibility for a distribution of bonding states (e.g., disilane). Absence of Raman scattering from the shiny areas of the sample at 27 GPa is consistent with metallic behavior (i.e., small penetration depth). If these regions are truly metallic, it is highly unlikely that they originate from gasket contributions. For gasket metal to migrate to the sample center, diffusion must take place on the order of 100 μm in 10 min, requiring a liquidlike diffusion coefficient—which is unreasonable for the gold. This suggests that silicon is a constituent of the metallic-looking phase; however, metal gasket materials may certainly catalyze this process in other cases.

We obtained Raman spectra during decompression to further characterize the highly reflective phase. At ~6 GPa the reflective region developed a measurable Raman spectrum in the low-frequency region near 400 cm^{-1}. Additionally, the free hydrogen present in the sample's black region disappeared and a new broad feature developed near 500 cm^{-1}. Figure 15 shows the details of these regions in the Raman spectra. The low-frequency contributions from the shiny region are identical to previously reported Raman spectra of decompressed metallic silicon.[75] These features were previously assigned to the *BC*8 and *R*8 structures,[75] and this metastable-back-transformation was also observed for germanium (*ST*12 structure).[76] Thus, we suggest that the reflective regions observed in the photomicrographs originate from metallic silicon and, by analogy, to the strikingly similar photos from the earlier study.[14] We suggest that metallic silicon can explain the abrupt changes in infrared reflectivity and electrical resistance associated with previous reports of metallization. The loss of Raman signal observed here during decomposition is similar to previous reports where silane was claimed to metallize.[14,16] The broad region that develops near 500 cm^{-1} is assigned to hydrogenated amorphous silicon based on consistency with thin-film literature.[77] Narayana *et al.*[19] observed similar spectra upon decompression of silane from 70 GPa as well as spectra from crystalline silicon without heating. The formation of partially hydrogenated amorphous silicon is consistent with the disappearance of the H-H vibron

with decreasing pressure as the partially decomposed silane is rehydrogenated in an amorphous state.

G. Superconductivity

Above, we have clearly demonstrated that in the absence of decomposition, SiH_4 is not metallic at pressures up to 150 GPa. At 55 GPa, where silane was previously reported to undergo an insulator-to-metal transition, we demonstrate that silane has a band gap >1 eV and appears orange in transmitted light. Additionally, the previously reported $P6_3$ metallic structure cannot be reconciled with theory and the consensus from first principles calculations indicates that the material with composition SiH_4 undergoes metallization above 200 GPa. How then can the previous report of superconductivity[16] be consistent with these results?

Degtyareva *et al.*[22] showed that the $P6_3$ phase is described well by platinum hydride (PtH_x). We acknowledge the possibility that PtH_x may exhibit a superconducting transition. Indeed, palladium hydride (PdH_x) is a known superconductor with T_c being a strong function of the hydrogen content x.[78,79] The magnitude of the transition temperature for the 1:1 PdH hydride [$T_c \sim 9$ K (Ref. 78)] at atmospheric pressure is similar to the transitions reported previously at high pressure.[16] The other obvious candidate for superconductivity is silicon. Above 12 GPa Si transforms into the metallic β-tin structure with a superconducting transition of ~4–6 K.[80–82] With increasing pressure, T_c of silicon passes through a maximum near 15 GPa (5–8 K) and decreases with further pressure increase.[80–82] A small rise in T_c at the hcp transition near 40 GPa was reported in one study.[82] T_c in silicon has not been measured above 45 GPa to our knowledge.

It is important to note that superconducting transitions in silicon depend strongly on the starting material and may also be influenced by sample history. Lin *et al.*[81] observed a systematic increase in T_c of ~3 K between 12 and 40 GPa when amorphous silicon was used as starting material instead of crystalline silicon. Extrapolation of T_c from these data to 60 GPa provides a $T_c \sim 6$ K, close to ~7 K reported by Eremets *et al.*[16] Berman *et al.*[83] measured amorphous hydrogenated silicon (α-Si:H) up to 20 GPa and observed anomalous behavior. T_c for the amorphous metallic phase initially decreased from ~7 K when pressure was increased above 10 GPa. The amorphous phase eventually crystallized with increasing pressure and developed a T_c of ~9 K. During pressurization between 14 and 18 GPa, they observed a metastable phase that could persist for several hours. Here, a slight increase in pressure caused T_c to increase by as much as 3 K. Notably, α-Si:H samples contained up to 16 at. % H and were produced through the decomposition of silane.[83]

Superconductivity of hydrogen-doped silicon in the crystalline and amorphous states should be explored further. It is now clear that a range of path-dependent states are accessible from silane, depending on sample history. A suite of amorphous, crystalline, and partially decomposed phases may be produced. In the absence of decomposition, SiH_4 clearly remains insulating (semiconducting) at pressures previously claimed for metallization. Our experimental observations agree well with theoretical studies, and true silane is neither metallic nor superconducting below ~200 GPa. However, the precarious nature of SiH_4 under pressure may be advantageous to producing novel materials with unique properties. In view of our results, and previous knowledge of superconductivity in hydrogenated silicon samples, we suggest that the superconductivity observed previously actually originates from partially hydrogenated silicon.

IV. CONCLUSIONS

The optical, electronic, and structural properties of silane (SiH_4) were examined to 150 GPa through the use of Raman spectroscopy, optical microscopy, synchrotron infrared reflectivity, optical absorption, and synchrotron x-ray diffraction measurements. Gold-lined sample gaskets were used to mitigate possible chemical reactions. Between 6 and 40 GPa the molecular, transparent, and insulating $P2_1/c$ was confirmed. Above ~40 GPa silane begins to darken under transmitted light. This darkening does not occur at a distinct pressure, but over a range, which suggests that initiation may be related to local sample stress. The darkening can be related to decomposition which may occur, especially after exposure to x rays or lasers. In the case of decomposition, samples are much more opaque and show a metallic luster. In the absence of decomposition, darkening is plausibly the result of a loss of molecular character with many enthalpically competitive pathways available contributing to the absorptive nature of the sample. Above 50 GPa, samples show a (partial) loss of crystallinity which may be consistent with amorphization or loss of molecular character, although no distinct diffuse x-ray scattering was observed. Above 100 GPa we observed crystallization into structures partially consistent with the previously reported nonmolecular $I\bar{4}2d$ and $I4_1/a$ types. In the absence of decomposition, silane remains partially transparent and nonmetallic to at least 150 GPa with a band gap constrained in the range of 0.6 to 1.8 eV. We suggest that previous reports of silane metallization are likely a consequence of decomposition and that superconductivity may originate from silicon or hydrogen-doped silicon that is not silane. While silane may readily decompose, this characteristic enables availability to a wide range of path- and sample-history-dependent metastable states and suggests a unique range of physical properties for hydrogen-rich silicon alloys.

ACKNOWLEDGMENTS

We acknowledge support from NSF-DMR (Grant No. DMR-085056), DOE/BES, DOE/NNSA (CDAC) and U.S. Army Research Office Grant No. 56122-CH-H. Portions of this work were performed at GeoSoilEnviroCARS (Sector 13), Advanced Photon Source (APS), Argonne National Laboratory. GeoSoilEnviroCARS is supported by the National Science Foundation–Earth Sciences (Grant No. EAR-0622171) and Department of Energy–Geosciences (Grant No. DE-FG02-94ER14466). Portions of this work were performed at HPCAT (Sector 16), Advanced Photon Source (APS), Argonne National Laboratory. HPCAT is supported by CIW, UNLV and LLNL through funding from DOE-NNSA, DOE-BES, and NSF. APS is supported by DOE-BES, under Contract No. DE-AC02-06CH11357. The U2A beamline is supported

by COMPRES, the Consortium for Materials Properties Research in Earth Sciences, under NSF Cooperative Agreement Grant No. EAR06-49658 and the US DOE (CDAC, Contract No. DE-AC02-98CH10886).

*tstrobel@ciw.edu

[1]K. Shimizu, H. Ishikawa, D. Takao, T. Yagi, and K. Amaya, Nature (London) **419**, 596 (2002).
[2]V. V. Struzhkin, M. I. Eremets, W. Gan, H. K. Mao, and R. J. Hemley, Science **298**, 1213 (2002).
[3]J. Nagamatsu, T. Nakagawa, T. Muranaka, Y. Zenitani, and J. Akimitsu, Nature (London) **410**, 63 (2001).
[4]E. Babaev, A. Sudbø, and N. W. Aschroft, Nature (London) **431**, 666 (2004).
[5]E. Wigner and H. B. Huntington, J. Chem. Phys. **3**, 764 (1935).
[6]N. W. Ashcroft, Phys. Rev. Lett. **21**, 1748 (1968).
[7]C. F. Richardson and N. W. Ashcroft, Phys. Rev. Lett. **78**, 118 (1997).
[8]P. Cudazzo, G. Profeta, A. Sanna, A. Floris, A. Continenza, S. Massidda, and E. K. U. Gross, Phys. Rev. Lett. **100**, 257001 (2008).
[9]N. W. Ashcroft, Phys. Rev. Lett. **92**, 187002 (2004).
[10]J. Feng, W. Grochala, T. Jaron, R. Hoffmann, A. Bergara, and N. W. Ashcroft, Phys. Rev. Lett. **96**, 017006 (2006).
[11]C. J. Pickard and R. J. Needs, Phys. Rev. Lett. **97**, 045504 (2006).
[12]Y. Yao, J. S. Tse, and K. Tanaka, Europhys. Lett. **78**, 37003 (2007).
[13]O. Degtyareva, M. Martinez-Canales, A. Bergara, X. J. Chen, Y. Song, V. V. Struzhkin, H. K. Mao, and R. J. Hemley, Phys. Rev. B **76**, 064123 (2007).
[14]X. J. Chen *et al.*, Proc. Natl. Acad. Sci. USA **105**, 20 (2008).
[15]R. P. Fournier, R. Sovoie, N. D. The, R. Belzile, and A. Cabana, Can. J. Chem. **50**, 35 (1972).
[16]M. I. Eremets, I. A. Trojan, S. A. Medvedev, J. S. Tse, and Y. Yao, Science **319**, 1506 (2008).
[17]X. J. Chen, J. L. Wang, V. V. Struzhkin, H. K. Mao, R. J. Hemley, and H. Q. Lin, Phys. Rev. Lett. **101**, 077002 (2008).
[18]D. Y. Kim, R. H. Scheicher, S. Lebegue, J. Prasongkit, B. Arnaud, M. Alouani, and R. Ahuja, Proc. Natl. Acad. Sci. USA **105**, 16454 (2008).
[19]C. Narayana, R. H. Greene, and A. L. Ruoff, J. Phys.: Conf. Ser. **121**, 042019 (2008).
[20]M. Martinez-Canales, A. R. Oganov, Y. Ma, Y. Yan, A. O. Lyakhov, and A. Bergara, Phys. Rev. Lett. **102**, 087005 (2009).
[21]Y. Yan, J. Gong, and Z. G. Zong, Chinese Phys. Lett. **27**, 017401 (2010).
[22]O. Degtyareva, J. E. Proctor, C. L. Guillaume, E. Gregoryanz, and M. Hanfland, Solid State Commun. **149**, 1583 (2009).
[23]N. Hirao, H. Fujihisa, Y. Ohishi, K. Takemura, and T. Kikegawa, in *Proceedings of International Symposium on Metal-Hydrogen Systems, Reykjavik, Iceland, 2008*; see also Acta. Cryst. **A64**, C609 (2008).
[24]M. Martinez-Canales, A. Bergara, J. Feng, and W. Grochala, J. Phys. Chem. Solids **67**, 2095 (2006).
[25]G. Gao, A. R. Oganov, A. Bergara, M. Martinez-Canales, T. Cui, T. Iitaka, Y. Ma, and G. Zou, Phys. Rev. Lett. **101**, 107002 (2008).
[26]Z. Li, W. Yu, and C. Jin, Solid State Commun. **143**, 353 (2007).
[27]C. Zhang, X. J. Chen, Y. L. Lin, V. V. Struzhkin, H. K. Mao, R. Q. Zhang, and H. Q. Lin, Europhys. Lett. **90**, 66006 (2010).
[28]J. S. Tse, Y. Yao, and K. Tanaka, Phys. Rev. Lett. **98**, 117004 (2007).
[29]G. Gao *et al.*, Proc. Natl. Acad. Sci. USA **107**, 1317 (2010).
[30]P. Gonzalez-Morelos, R. Hoffmann, and N. W. Ashcroft, ChemPhysChem **11**, 3105 (2010).
[31]P. Zaleski-Ejgierd, R. Hoffmann, and N. W. Ashcroft, Phys. Rev. Lett. (in press, 2011).
[32]I. Goncharenko, M. I. Eremets, M. Hanfland, J. S. Tse, M. Amboage, Y. Yao, and I. A. Trojan, Phys. Rev. Lett. **100**, 045504 (2008).
[33]D. Y. Kim, R. H. Scheicher, H. K. Mao, T. W. Kang, and R. Ahuja, Proc. Natl. Acad. Sci. USA **107**, 2793 (2010).
[34]X. Jin *et al.*, Proc. Natl. Acad. Sci. USA **107**, 9969 (2010).
[35]D. Y. Kim, R. H. Scheicher, and R. Ahuja, Phys. Rev. Lett. **103**, 077002 (2009).
[36]E. Zurek, R. Hoffmann, N. W. Ashcroft, A. R. Oganov, and A. O. Lyakhov, Proc. Natl. Acad. Sci. USA **106**, 17640 (2009).
[37]D. Duan *et al.*, J. Chem. Phys. **133**, 074509 (2010).
[38]G. Markopoulos, P. Kroll, and R. Hoffmann, J. Am. Chem. Soc. **132**, 748 (2010).
[39]J. S. Tse, Z. Song, Y. Yao, J. S. Smith, S. Desgreniers, and D. D. Klug, Solid State Commun. **149**, 1944 (2009).
[40]T. A. Strobel, M. Somayazulu, and R. J. Hemley, Phys. Rev. Lett. **103**, 065701 (2009).
[41]S. B. Wang, H. K. Mao, X. J. Chen, and W. L. Mao, Proc. Natl. Acad. Sci. USA **106**, 14763 (2009).
[42]T. A. Strobel, X. J. Chen, M. Somayazulu, and R. J. Hemley, J. Chem. Phys. **133**, 164512 (2010).
[43]Y. Li, G. Gao, Y. Xie, Y. Ma, and G. Zou, Proc. Natl. Acad. Sci. USA **107**, 15708 (2010).
[44]M. Ramzan, S. Lebegue, and R. Ahuja, Phys. Rev. B **81**, 233103 (2010).
[45]Y. Li, G. Gao, Q. Li, Y. Ma, and G. Zou, Phys. Rev. B **82**, 064104 (2010).
[46]X. Q. Chen, S. Wang, W. L. Mao, and C. L. Fu, Phys. Rev. B **82**, 104115 (2010).
[47]Y. Yao and D. D. Klug, Proc. Natl. Acad. Sci. USA **107**, 20893 (2010).
[48]W. L. Yim, J. S. Tse, and T. Iitaka, Phys. Rev. Lett. **105**, 215501 (2010).
[49]K. Michel, Y. Liu, and V. Ozolins, Phys. Rev. B **82**, 174103 (2010).
[50]H. K. Mao, J. Xu, and P. M Bell, J. Geophys. Res. **91**, 4673 (1986).
[51]O. L. Anderson, D. G. Isaak, and S. Yamamoto, J. Appl. Phys. **65**, 1534 (1989).
[52]Y. Akahama and H. Kawamura, J. Appl. Phys. **100**, 043516 (2006).
[53]A. P. Hammersley, ESRF Internal Report, ESRF97HA02T, "FIT2D: An Introduction and Overview" (1997).
[54]M. Fox, *Optical Properties of Solids* (Oxford University Press, Oxford, 2010).
[55]C. T. Seagle, W. Zhang, D. L. Heinz, and Z. Liu, Phys. Rev. B **79**, 014104 (2009).
[56]*CRC Handbook of Chemistry and Physics*, edited by D. R. Linde (CRC Press, Boca Raton, FL, 2004).
[57]R. J. Hemley, H. K. Mao, L. W. Finger, A. P. Jephcoat, R. M. Hazen, and C. S. Zha, Phys. Rev. B **42**, 6458 (1990).
[58]H. Olijnyk, S. K. Sikka, and W. B. Holzapfel, Phys. Lett. A **103**, 137 (1984).

[59]M. I. McMahon, R. J. Nelmes, N. G. Wright, and D. R. Allan, Phys. Rev. B **50**, 739 (1994).
[60]E. W. Lemmon, M. O. McLinden, and D. G. Friend, NIST Chemistry WebBook, NIST Standard Reference Database No. 69, edited by P. J. Linstrom and W. G. Mallard, Gaithersburg, MD, 2010.
[61]H. Hermes, A. Driessen, and R. Griessen, J. Phys. C **19**, 3571 (1986).
[62]M. Sakashita, H. Fujihisa, H. Yamawaki, and K. Aoki, J. Phys. Chem. A **104**, 838 (2000).
[63]H. Fujihisa, H. Yamawaki, M. Sakashita, A. Nakayama, T. Yamada, and K. Aoki, Phys. Rev. B **69**, 214102 (2004).
[64]G. R. Hearne, M. P. Pasternak, and R. D. Taylor, Phys. Rev. B **52**, 9209 (1995).
[65]A. L. Chen, P. Y. Yu, and M. P. Pasternak, Phys. Rev. B **44**, 2883 (1991).
[66]M. P. Pasternak, R. D. Taylor, M. B. Kruger, R. Jeanloz, J. P. Itie, and A. Polian, Phys. Rev. Lett. **72**, 2733 (1994).
[67]N. Hamaya, K. Sato, K. Usui-Watanabe, K. Fuchizaki, Y. Fujii, and Y. Ohishi, Phys. Rev. Lett. **79**, 4597 (1997).
[68]S. J. Duclos, Y. K. Vohra, and A. L. Ruoff, Phys. Rev. B **41**, 12021 (1990).
[69]M. Hanfland, J. E. Proctor, C. L. Guillaume, O. Degtyareva, and E. Gregoryanz, Phys. Rev. Lett. **106**, 095503 (2011).
[70]K. A. Goettel, J. H. Eggert, I. F. Silvera, and W. C. Moss, Phys. Rev. Lett. **62**, 665 (1989).
[71]T. Kume, Y. Fukaya, S. Sasaki, and H. Shimizu, Rev. Sci. Instrum. **73**, 2355 (2002).
[72]S. Endo, A. Honda, S. Sasaki, H. Shimizu, O. Shimomura, and T. Kikegawa, Phys. Rev. B **54**, 717 (1996).
[73]J. Tauc, R. Grigorovici, and A. Vancu, Phys. Status Solidi. **15**, 627 (1966).
[74]See supplemental material at [http://link.aps.org/supplemental/10.1103/PhysRevB.83.144102] for decomposition images.
[75]H. Olijnyk and A. P. Jephcoat, Phys. Status Solidi B **211**, 413 (1999).
[76]F. Coppari, J. C. Chervin, A. Congeduti, M. Lazzeri, A. Polian, E. Principi, and A. Di Cicco, Phys. Rev. B **80**, 115213 (2009).
[77]C. Smit, R. A. C. M. M. van Swaaij, A. M. H. N. Petit, W. M. M. Kessels, and M. C. M. van de Sanden, J. Appl. Phys. **94**, 3582 (2003).
[78]R. J. Miller and J. C. Satterthwaite, Phys. Rev. Lett. **34**, 144 (1975).
[79]I. S. Balbaa, A. J. Pindor, and F. D. Manchester, J. Phys. F **14**, 2637 (1984).
[80]K. J. Chang, M. M. Dacorogna, M. L. Cohen, J. M. Mignot, G. Chouteau, and G. Martinez, Phys. Rev. Lett. **54**, 2375 (1985).
[81]T. H. Lin, W. Y. Dong, K. J. Dunn, C. N. J. Wagner, and F. P. Bundy, Phys. Rev. B **33**, 7820 (1986).
[82]D. Erskine, P. Y. Yu, K. J. Chang, and M. L. Cohen, Phys. Rev. Lett. **57**, 2741 (1986).
[83]I. V. Berman, N. B. Brandt, I. L. Romashkina, V. I. Sidorov, V. A. Alekseev, Zh. Eksp. Teor. Fiz. **41**, 288 (1985) [JETP **41**, 353 (1985)].